IEEE Access
Multidisciplinary | Rapid Review | Open Access Journal

Received October 16, 2020, accepted October 26, 2020, date of publication October 28, 2020, date of current version November 12, 2020.

Digital Object Identifier 10.1109/ACCESS.2020.3034366

Design and Implementation of an OCC-Based Real-Time Heart Rate and Pulse-Oxygen Saturation Monitoring System

MD. FAISAL AHMED, (Graduate Student Member, IEEE), MOH. KHALID HASAN, (Member, IEEE), MD. SHAHJALAL, (Student Member, IEEE), MD. MORSHED ALAM, (Graduate Student Member, IEEE), AND YEONG MIN JANG, (Member, IEEE)

Department of Electronics Engineering, Kookmin University, Seoul 02707, South Korea

Corresponding author: Yeong Min Jang (yjang@kookmin.ac.kr)

This work was supported in part by the Ministry of Science (MSIT) and Information and Communication Technology (ICT), South Korea, through the Information Technology Research Center (ITRC) Support Program, supervised by the Institute for Information & Communications Technology Promotion (IITP) under Grant IITP-2018-0-01396, in part by the Institute for Information and Communications Technology Promotion (IITP) Grant through the Korea Government (MSIT) under Grant 2017-0-00824, and in part by the Development of Intelligent and Hybrid Optical Camera Communication-Light Fidelity (OCC-LiFi) Systems for Next Generation Optical Wireless Communications.

ABSTRACT In this technical paper, we design and implement an optical camera communication system for real-time remote monitoring of patient's heart rate (HR) and oxygen saturation (SpO_2) data. The data is collected and transmitted by a patch circuit which comprises a MAX30102 sensor and an RGB LED array. A close circuit television camera is used not only for surveillance but also for receiving the data simultaneously. The LED is modulated using color intensities, and the data can be retrieved regardless of any orientations of the LED array. We propose a neural network (NN) to detect each LED separately, and we implement another NN-based on feature extraction to precisely recognize the colors. The data are also encoded with a unique key, which increases the security of the communication mechanism. System performance of 4.68 kbps with low bit-error-rate (BER) and 1.172 kbps with moderate BER is achieved at 1 and 3 m, respectively.

INDEX TERMS Optical camera communication (OCC), image processing, neural network (NN), remote patient monitoring.

I. INTRODUCTION

One of the most significant diagnostic tests in clinical medicine is the measurement of heart rate (HR) and blood oxygen saturation (SpO_2), which can effectively determine the physiological state of the human body [1]. Therefore, it is crucial to monitor these healthcare data, especially in such a period when the world is immobilized by disastrous contagious diseases like COVID-19, in which more than 35 million people were affected across 213 countries, as of this writing [2]. The status of HR and SpO_2 levels is incredibly significant not only for a disease like COVID-19 but also for any serious malady related to the human circulatory and respiratory system. In consideration of this health information, designing a reliable real-time monitoring system has attracted significant research interest recently.

The healthcare data are collected using a wearable sensor connected to a communication device to provide healthcare services across the users. The transmission of health information can be done wired and wireless. Wired-connected sensors are odd, costly, and consume high power. On the other hand, currently, radio-frequency (RF)-based devices, such as Bluetooth, ZigBee, and 6LowPAN are mostly used for wireless communication objectives. However, it can cause serious damage to human health and negative biological effects in the human body when long-term involvement with electromagnetic radiation (EMR) originating for RF [3]–[6]. In addition, medicinal devices are very sensitive to EMR, and its continuous usage can gradually deteriorate the performance of medical instruments [7], [8]. Furthermore, for being

The associate editor coordinating the review of this manuscript and approving it for publication was Shuping He.

omnidirectional, RF devices are not secured, and the signals are often affected by inter-channel interferences, which eventually questions the reliability. Therefore, the necessity of a suitable technology to use as a complementary or replacement of RF-based devices cannot be overlooked.

In this study, we propose an optical camera communication (OCC) system to transmit data. Generally, OCC is a line-of-sight (LoS) technology that uses an LED as a transmitter, a camera image sensor as a receiver, and visible light as the communication medium. OCC supports several constructive characteristics such as low cost, high security, low power consumption, and enhanced reliability. Because the system uses visible light, it is free from electromagnetic interferences and completely risk-free to human health [9].

In this work, we have designed and implemented a complete end-to-end system for real-time monitoring of patient's HR and SpO_2 data, in which we have used a pulse oximeter sensor, MAX30102, to collect the infrared (IR), bit-per-minute (BPM), and SpO_2 data from the patient's body. A microcontroller is used to receive the photoplethysmogram (PPG) signals and the BPM data that are further exploited to generate the ECG signals. A 4×4 RGB LED array is modulated with the data using color intensity modulation (CIM) [10]. A patch circuit mountable in the patient's hand is designed integrating the LED array and the microcontroller. Neural networks (NNs) are developed to detect and recognize each LED and its color in the LED array using a close circuit television (CCTV) camera, which is also used for the surveillance objective, simultaneously. The data are decoded and processed in real-time in Python 3.7 and sent to a cloud server.

Previous studies discussed the application of OCC in health monitoring [11], [12]. However, none of them are implementation-based work; rather, only simulations were considered. In [13], OCC was applied to monitor humidity, temperature, and CO_2 using RGB LED [13]; however, the achieved data rate was very low (8–30 bps). In [14], an NN-based OCC system was proposed for monitoring weather conditions, in which substantial data rate and an excellent bit-error-rate (BER) were achieved; however, the demonstration of their scheme was only at 50 cm. To the best of the authors' knowledge, this is the first report to design a complete end-to-end OCC-based health monitoring system, where the whole procedure from data acquisition from the sensor to storing the data in a cloud server is demonstrated. For being directional, OCC is a secured communication system; however, if the modulation and encoding procedure is certain, using another camera can retrieve the data. Therefore, to increase security, we have also implemented a model by adding a unique key at the transmitter. No security protocol has been proposed for OCC until now. In [15], a security protocol using a camera was proposed; however, the communication system was designed using photodiode (PD) with different channel matrices. Furthermore, the data can be erroneous if a different row of the projected image of the LED array is captured first as we are using the intensity of the LED for recognizing the color. We have proposed a technique to resolve the orientation issue. In [16], the authors also invested efforts to solve the orientation problem; however, the achieved communication distance was only 30 cm.

Recently, designing a reliable real-time health monitoring system is extensively researched. The most considered healthcare information includes HR, SpO_2 level, blood pressure, and body temperature [17]–[20]. Reducing power consumption is the main reason to use wireless technology for healthcare data transmission. The most adopted wireless systems are Bluetooth and ZigBee [1], [21]. In this study, to collect the HR and SpO_2 data, we have used a pulse oximeter sensor, which was used in previous studies [22], [23]; however, in [22], two Bluetooth modules were used, whereas in [23], a costly processor was used. In [24], a health monitoring system was developed, where IR rays were emitted into the patient's organ, which was captured using a camera, and the image was processed to collect the SpO_2 data. However, the system was too costly, consumes high power, and provides high error in the measured data. On the other hand, we have used an LED array as transmitter, which is cost-effective and supports low-power consumption, and a CCTV camera as receiver, which is almost installed in every clinic. In brief, the contributions of this study are listed as follows.

1) For real-time remote monitoring of the patient's ECG (generated from IR and BPM values) and oxygen saturation level, a patch-based OCC system is designed using an RGB LED array as transmitter and a CCTV camera as receiver. The CCTV camera used in the system can be utilized for both communication and surveillance, simultaneously.
2) A data-retrieval mechanism using CIM is developed, and a technique is proposed to consider any orientation of the LED array.
3) An NN-based LED detection mechanism is proposed, where each LED in the LED array is detected separately. A feature extraction-based NN is also designed for precise color recognition.
4) To enhance security in the communication system, an encryption scheme is proposed. After processing, the data is transmitted to a server that can be accessed by an authorized person.

The rest of the paper is organized as follows. Section II presents an overview of the proposed scheme. The detailed explanation of the system is provided in Section III. Section IV includes the experimental results and a discussion of the research findings. Finally, the paper is concluded in Section V.

II. OVERVIEW

In this work, an indoor scenario is considered, wherein a patient's health is continuously monitored. Using a sensor fixed in a finger of the patient, we collected the patient's healthcare data, specifically the HR and SpO_2 data. The sensor is connected with a patch circuit attached as an armband in

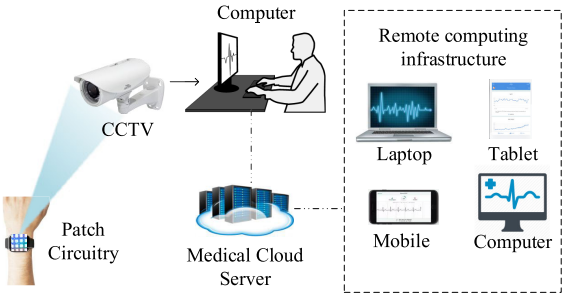

FIGURE 1. Overview of the proposed health monitoring system.

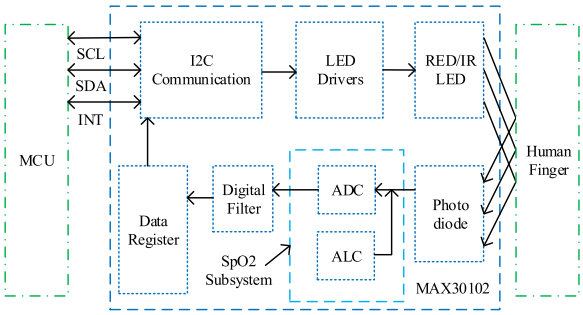

FIGURE 2. Functional block diagram of the sensor connected to the human body and the microcontroller.

the patient's body. The patch is composed of an LED array, modulated using the sensing data. A CCTV camera is used for surveillance and receiving data from the LED array using OCC simultaneously. Afterward, the data are processed and accessed in real-time by the remote monitor. Simultaneously, the data are transmitted to a cloud server, which can be further accessed by any authorized person using a private user ID and password. Figure 1 shows a block diagram of the proposed system.

III. SYSTEM DESIGN

The developed patch comprises a pulse oximeter sensor, a microcontroller, and an RGB LED array. The optical sensor and the RGB LED array are controlled by the microcontroller so that the data sensed from the human body are processed, modulated, and driven to the LED array. Figure 2 shows the overall architecture of the patch and a setup scenario in the human body. Then, the optical signal from the LED array is transmitted to the camera and the server subsequently. The rest of the section discusses the healthcare data sensing, the communication system, data reconstruction and processing, and the security protocol.

A. OPTICAL SENSING AND DATA ACQUISITION

To garner the SpO_2 and HR information from the human body, we used a MAX30102 sensor, which is a complete pulse oximetry and heart rate sensor module designed for the demanding requirements of wearable devices. The sensor is very small in size that could collect data without sacrificing optical or electrical performance. Figure 2 shows the complete functional diagram. An LED driver is integrated to modulate the Red and IR LEDs, and a PD is used to receive the optical signals. The sensor includes an SpO_2 subsystem containing an ambient light cancellation unit (ALC), a continuous-time sigma-delta (ADC), and a proprietary discrete-time filter. The sensor also has an on-chip temperature sensor that calibrates the temperature dependency of the SpO_2 subsystem. For further reading and writing the data, the sensor utilizes a data register and an I^2C communication bus. The I^2C line uses several bus wires, such as serial data wire (SDA), serial clock wire (SCL), and active-low interrupt (INT) to drive the data to the microcontroller (MCU).

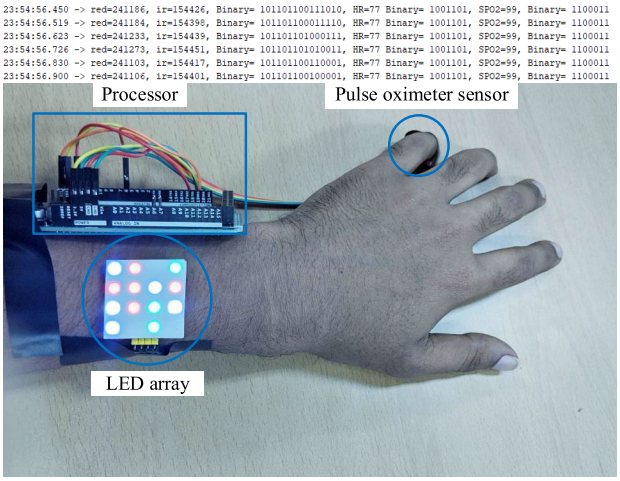

FIGURE 3. The input data, and the patch architecture and its setup scenario in the human body.

B. OCC PROTOTYPE

1) TRANSMITTER

In the microcontroller, the data are processed through several steps before steering to the LED array. The microcontroller continuously communicates with the I^2C bus and generates three decimal bitstreams from the data, which contain IR, HR, and SpO_2 data, respectively. The PPG signal is collected from the patient's finger and processed using the SpO_2 algorithm, a sampling rate of 100 Hz, a pulse width of 411 μs, and an ADC range of 4096-bit. The bitstreams pass through a serial-to-parallel converter after transforming to the binary form. If the binary bitstreams are not divisible by the number of bits per symbol, few additional zeros are added at the beginning of the bitstream. The data are then modulated using the CIM scheme, which is mainly a combination of the color-shift keying and the pulse amplitude modulation techniques. In this scheme, the data are mapped into the color and intensity of each LED. The LED array has 16 LEDs, each with an individual symbol and four colors (white, red, blue, and green). On the basis of the length of the bit sequence, the IR, BPM, and SpO_2 data are assigned to the first eight LEDs, the second four LEDs, and the final four LEDs in the 4×4 matrix, respectively. The last LED for each type of data is kept "OFF", as shown in Figure 3. The ending of each

data stream is indicated by these three OFF LEDs, therefore, mitigating the necessity of any header, footer, or flag bits and increasing the bit efficiency. In addition, the three bits are also used for assuaging the effect of unwanted orientation of the transmitter, which is further explained in Section 3.B(3). Before assigning the LED for data transmission, the data are transformed into another coded form for obtaining a secure protocol that is explained in Section 3.B(6).

2) DATA RECEIVING AND COLOR RECOGNITION

A Bayer pattern filter is used to recognize the color when the optical signal befell on the image sensor; thus, a color image is formed. Half of the filter is composed of green filter, whereas the other two quarters are composed of red and blue filters. To recognize the LED region inside the image, we controlled the exposure time after constructing an image. Afterward, the edges of the LED region are selected, and an offset value is added to all the pixel coordinates of the edges, consequently generating a boundary containing only the LED image, which is further resized to keep the aspect ratio constant. How much the size of the LED image augmented depends on the actual size of the LEDs inside the image sensor. However, the image experiences blurriness and distortion because of the magnification. By filtering, resampling, and smoothing, we resolved the blur effect. On the other hand, using an NN-based super-resolution technique, we remediated the image distortion. In this regard, 60% of the total acquired image are trained, and in the training process, a file called FSRCNN_x2.pb is used as the weight configuration.

To detect each LED in the 4×4 matrix, we used another NN after getting the unblemished image. Darknet and OpenCV are used in the Python 3.7 platform to train the images. The weight configurations of the trained images are used in the test images to detect and label each LED. However, a variation in the color intensity is observed between pixels of each detected LED. Therefore, it is challenging to conclude a specific color code for each LEDs. As a solution, we developed an NN-based feature extraction technique for each pixel. Each color has unique features depending on the grayscale code of the R, G, and B, which are further commingled to form different vectors.

Afterward, the vectors are assigned in a group for a specific color. Depending on the variations of a certain part of the vectors, different weight values are generated, which are further assigned to the hidden layer of the NN. The NN is applied thenceforth to the previously detected pixels, and the color code of each pixel is eventually determined using the weight values trained beforehand. Finally, using the confirmed color codes of each LED, we have constructed a 4×4 matrix, which is also used to extract the original data. On the basis of the matrix coordinates, the elements are assigned consecutively in the matrix; therefore, the OFF LED locations are kept blank. Figure 4 shows the whole color recognition process.

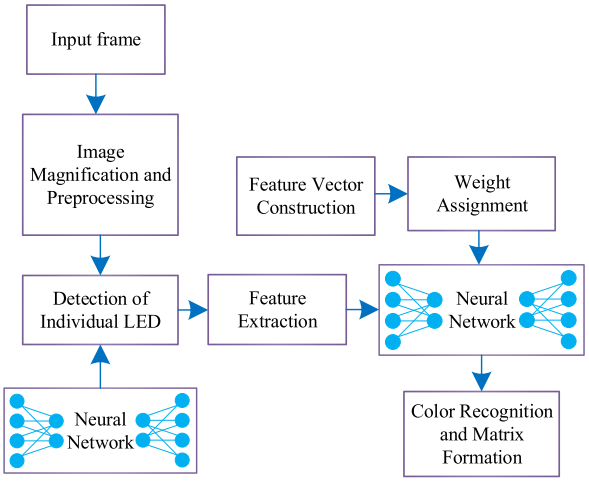

FIGURE 4. The receiving architecture with color recognition and matrix formation.

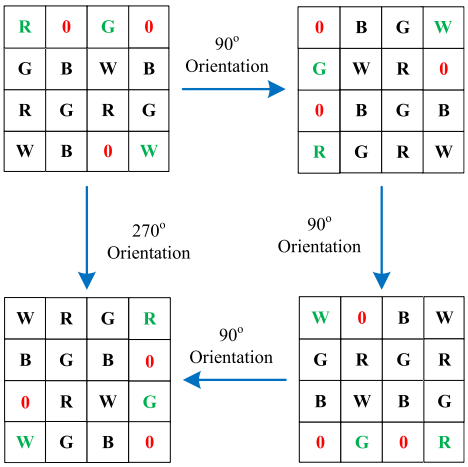

FIGURE 5. Four possible orientations of the 4 × 4 LED matrix.

3) DATA DECODING

The retrieval of the received signal significantly depends on the orientation of the transmitter. It will not be sophisticated to maintain a fixed position of the patch as the placement of the hand may be altered on the basis of the patients' requirements. However, different orientations of the LED array will generate substantial errors in the data. By measuring the amount of inflection of the LED array, we have avoided the challenge. Figure 5 shows different orientations of the LED array compared with the original image. As mentioned in Section 3.B(1), three LEDs are reserved in the OFF position to indicate the starting and ending points of each IR, BPM, and SpO_2 data. The three positions will be unchanged in the LED matrix, disregarding any inflection. Thus, in the original LED matrix, the amount of orientation is calculated to locate the positions of the OFF LEDs. The data may vary significantly; thus, any other LEDs can progress in the OFF state if the data are too small. However, as we defined the OFF LEDs at the end of each dataset, the newly OFF LEDs will appear sequentially just before the specific OFF LED, determining the positions of the OFF LEDs easily. The starting point of the

dataset is defined after measuring the inflection angle. Then, the symbols are decoded using the color code sequence in the LED matrix. Finally, the data for IR, BPM, and SpO_2 are stored into three separate CSV files.

4) EFFECT OF CHANNEL PROPERTIES

Background noise and interference from the neighboring light sources can affect the OCC performance. The intensity of the background light can have a significant effect on the change in the intensity level of the RGB LED. This type of noise is realized on a scale of 0 and 1, where a value of 0 is associated with an ideal situation with no ambient light, whereas a value of 1 indicates a fully noisy image from which no data can be extracted and no reliable tracking can be performed. After controlling the exposure time, we could extract the data properly.

The camera receives red, green, and blue, forming an image containing the colored data distorted by the channel background noise. However, because of the discrete nature of the digital image generated at the image sensor, the intensity values over each of the red, green, and blue channels of the received image cannot exceed a certain threshold. This threshold is typically 255, as each pixel is represented by an eight bits value, and is often normalized. Effectively, any signal with noise non-linearity above a certain level will be mapped to a value for that particular pixel. The threshold should be below 128 so that the pixel could show the different R, G, B.

Besides the background noise non-linearity, the path loss is to be taken into account to prepare the data distortion model over the channel, capturing the effect of the distance and the angle between the transmitter and the receiver. Besides affecting the intensity of the non-linearity of noise received, these variations affect the code of the data. Decreasing the size of the detected rectangle due to a long-distance between the transmitter and receiver or reducing the intensity of the received color makes the data more variable to the noise, which could result in higher BER values.

5) ECG SIGNAL CONSTRUCTION

To fabricate the ECG signal, we used the IR and BPM data. The whole signal processing is performed on the basis of the Pan Tompkins algorithm. To generate the curves, we have taken the average of every 100 samples of the BPM value. On the other hand, to present the slop more precisely, every single interval of the IR data is utilized after adding an offset. To form the waveform of the ECG signal, we followed the following steps.

1) First, the program takes the raw IR signal in a fixed time interval. After that, the data are filtered out using a bandpass (1–30 Hz) filter (composite of high and low pass filters).
2) Next, the sharp peaks, the nadirs of the QRS, and the notches are differentiated to integrate the signal with the IIR filter at 60 Hz.

TABLE 1. Experimental parameters.

Parameters	Values
Room size	$5 \times 4 \times 3$ m
Maximum distance	3 m
Camera frame rate	30 fps
Image resolution	1280×720 pixels
LED type	4×4 RGB LED matrix
Sensor type	MAX30102
Frequency	2 kHz
Exposure time	1.25 ms
Number of color used	2, 4, and 8

3) Then, after integrating the derivative of the signal with the moving window, a threshold is set to find the precise peak. Therefore, the peak is properly recognized, and the QRS complex is estimated.

Finally, the output of the ECG signal is generated and the number of peaks is plotted using the BPM information.

6) PROPOSED SECURITY PROTOCOL

After approaching the LED access point, a camera can retrieve the data if the process of encoding the data is certain and have the proper decoding mechanism and intrinsic properties. Medical data can be sensitive; therefore, we have proposed a unique key that is only valid for a specific user. The main data pattern is updated to a coded form in the transmitter when using a key. Let us assume that the original input signal is x, which is formed using several symbols, and then each symbol is constructed as a form of triplets.

$$x = \{s_1, s_2, \ldots, s_N\} \tag{1}$$

where

$$s_n = \left[i_r^n \; i_g^n \; i_b^n\right] \tag{2}$$

The i_r^n, i_g^n, and i_b^n denote the peak currents of the red, green, and blue LEDs, respectively, considering the nth symbol. The received signal by the image sensor will be as follows:

$$\mathbf{r} = \mathbf{H}\mathbf{x} + \mathbf{n} \tag{3}$$

where $\mathbf{H}$ and $\mathbf{n}$ are the optical channel gain and noise in matrix form, respectively. Now, we convert the input signal $\mathbf{x}$ into a coded signal $\mathbf{o}$ which will be sent by the LED access point; $\mathbf{o}$ is generated using the unique key k_p and constructed with four parts (k_1, k_2, k_3, and k_4), where each part is composed as

$$k_{p\epsilon[1,4]} = \left[i \; j \; k\right] \tag{4}$$

where i, j, and k are octets whose value range from 0-255. It is worth noting here that the values of $\mathbf{x}$, $\mathbf{c}$, and $\mathbf{c_I}$ range from 0-255. In addition, the output signal also varies from 0-255. However, the addition of $\mathbf{x}$ and $\mathbf{c}$ can exceed 255, therefore, their average is multiplied by $\mathbf{c_I}$ and then divided by 255. Now, $\mathbf{x}$ is converted in a 4×4 matrix and $\mathbf{o}$ is presented as

$$\mathbf{o} = 0.00196\,(\mathbf{x} + \mathbf{c})\,\mathbf{c_I} \tag{5}$$

TABLE 2. The mean absolute error of the sensor data in different situation.

	Situation	Blood oxygen saturation (MAE)	Heart rate (MAE)
Night	Interference from a light source with low intensity	0.12	0.16
Night	Interference from multiple light sources	0.60	0.63
Day	Interference from sunlight only	0.47	0.46
Day	Interference from sunlight and multiple light sources	0.71	0.75

where $\mathbf{c} = \begin{bmatrix} k_1 & k_1 & k_1 & k_1 \\ k_2 & k_2 & k_2 & k_2 \\ k_3 & k_3 & k_3 & k_3 \\ k_4 & k_4 & k_4 & k_4 \end{bmatrix}$ and $\mathbf{c_I}$ is the multiplication of $\mathbf{c}$ and a 4×4 identity matrix. Therefore, using the value of $\mathbf{o}$, Eq. 5 is updated as

$$\mathbf{r} = 0.00196\mathbf{H}\left(\mathbf{x} + \mathbf{c}\right)\mathbf{c_I} + \mathbf{n} \tag{6}$$

When the camera receives the data, the noise and interferences can be removed using different filtering techniques. Finally, the data is demodulated using the following equation:

$$\mathbf{x} = 510\left(\mathbf{r} \times \mathbf{H}^{-1}\right)\mathbf{c_I^{-1}} - \mathbf{c} \tag{7}$$

IV. PERFORMANCE ANALYSIS

Experiments are conducted to assess the proposed OCC based remote monitoring system. An IP camera (DH-IPCHFW1230SP-036 –1080p 3.6 mm DAHUA) was used in the experiment, and Python 3.7 was used to detect the LED and decode and process the data. Table 1 shows the implementation parameters. Figure 6(a) shows a specific frame received by the camera, whereas Figure 6(b) depicts the processed figure for OCC. To detect each LED separately, we need to control the exposure time of the camera. The image frames are also used for surveillance; however, it is not possible to use two different exposure times simultaneously. Therefore, firstly, we have controlled the brightness of each image frame to use for the surveillance. Concurrently, each image frame is processed with increasing adequate resolution to the projected LED region.The output at the receiver is also illustrated in Figure 6(b).

Each LED in the 4 × 4 matrix is detected separately using the NN, and a data rate of 4.68 kbps is achieved, which can be further augmented by using a camera with a higher frame rate. Figure 7 shows the BER performance of the proposed scheme. If the color intensity is increased, the accuracy of the LED detection will be increased, thus reducing the BER. Fortunately, we could achieve the maximum normalized intensity when the transmit power is set to 3.3 W, consequently achieving a BER around 10^{-6} at a communication distance of 1 m. The number of colors has a profound impact on the

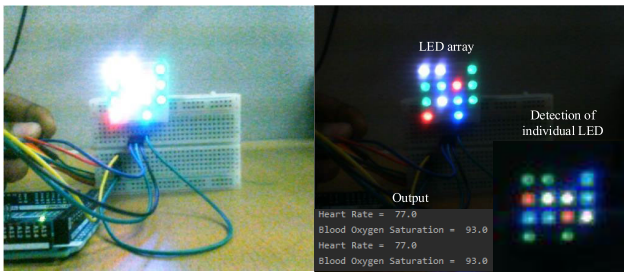

FIGURE 6. (a) An image of the implemented 4 × 4 LED matrix (b) the detection of each LED separately and the output after processing.

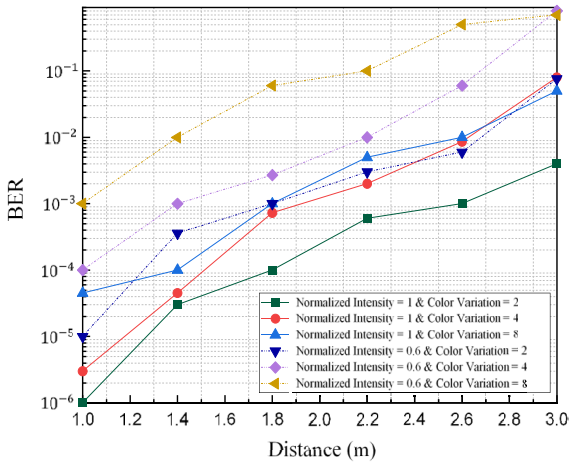

FIGURE 7. The effect of BER with respect to the distance considering the effect of normalized intensity and number of different colors are used.

OCC performance: the higher the number of colors, the lower the accuracy of color detection, resulting in higher BER. As discussed in Section 3, the data are composed of three different types (IR, BPM, and SpO_2), which are collected in three different CSV files. However, several sudden spikes are observed in the data. The larger spikes are eliminated using a filter, whereas the smaller ones are removed using the sliding window mechanism considering a particular window size. The IR data for around 1100 samples is shown in Figure 8(a), and the ECG signals generated using 64 BPM from the IR data is shown in Figure 8(b). Using a Butterworth and infinite-impulse-response notch filter, we executed the ECG feature extraction algorithm to the IR data. We then performed the first derivative of the signal using a Lagrange five-point interpolation formula and then computed the Hilbert transform of those samples. The whole signal generation procedures are performed in Python 3.7.

On the other hand, the SpO_2 and the BPM data are plotted in Figure 9. We have taken 400 samples to generate the graphs. As shown in the figure, several unstable spikes are generated within the initial samples. The reason is the initial stirs of the patch while attaching the sensor. The exact BPM and SpO_2 values can be observed after 125 and 200 samples, respectively. The experiments are performed on a 26-year-old male volunteer whose weight is 62 kg and height is 167 cm. Table 2 gives information on mean absolute error (MAE)

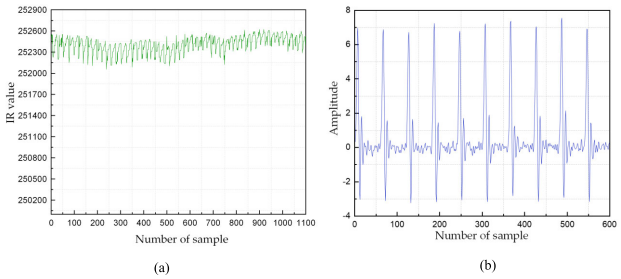

FIGURE 8. (a) The output PPG signal before filtering (b) the generated ECG signal by taking the BPM value as 64.

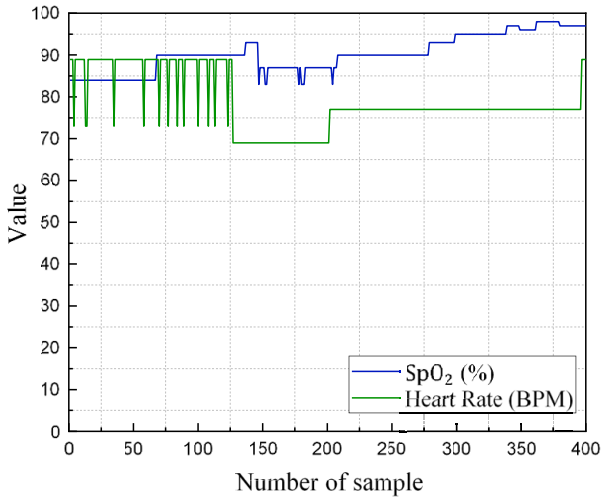

FIGURE 9. The value of blood oxygen saturation and heart rate with respect to the number of sample in the output.

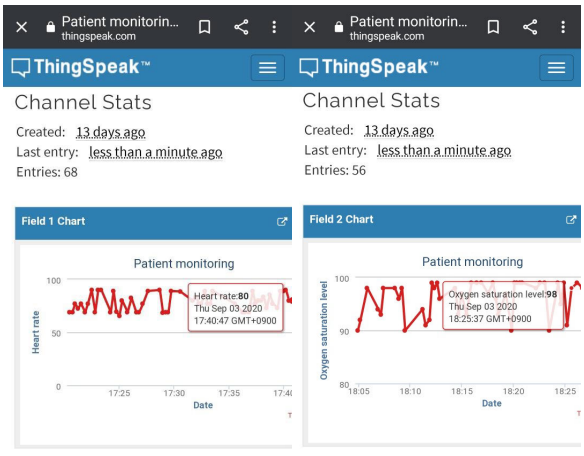

FIGURE 10. Data (HR and SpO_2) monitoring accessing the cloud server using smartphone.

of the data of the volunteer in different lighting conditions. We consider four different indoor conditions. Firstly, in the nighttime, the data are taken using multiple room light sources and a single light source with low intensity, separately. The same procedure is applied in the daytime using slight sunlight entering the room. It can be seen that the MAE increases when the interferences are high. Finally, as shown in Figure 10, the data are sent to an IoT cloud server where an authorized person can access the data using a login ID and password.

V. CONCLUSION

In this study, we proposed a real-time health monitoring system based on OCC where a MAX30102 sensor was used to collect the IR, SpO_2, and BPM data and connected to a patch mounted on the patient′s hand. The patch was composed of an LED array used to transmit the data to a CCTV camera. The LED array was modulated using CIM and the data were encoded with a unique key to enhance the security. Each LED in the array was detected using an NN, and another feature-extraction-based NN was used to recognize the colors precisely. A mechanism was also developed to assuage the challenge of different LED array orientations in the decoding procedure. Finally, the data were processed and accessed by a remote monitor and stored in a cloud server. A data rate of 4.68 kbps and an excellent BER were achieved, demonstrating the reliability of the remote monitoring system.

REFERENCES

[1] B. Jiao, "Anti-motion interference wearable device for monitoring blood oxygen saturation based on sliding window algorithm," *IEEE Access*, vol. 8, pp. 124675–124687, 2020.
[2] Covid-19 coronavirus pandemic. *Worldometer*. Accessed: Oct. 3, 2020. [Online]. Available: https://www.worldometers.info/coronavirus/
[3] Radiofrequency (RF) Radiation, USA. *Health physics society*. Accessed: Oct. 3, 2020. [Online]. Available: https://hps.org/hpspublications/articles/rfradiation.html
[4] Non-ionizing Electromagnetic Radiation in the Radiofrequency Spectrum and Its Effects on Human Health. *Latin America*. Accessed: Oct. 3, 2020. [Online]. Available: http://www.wireless-health.org.br/downloads/LatinAmericanScienceReviewReport.pdf
[5] L. Rsa and M. Ga, "Effects of wireless devices on human body," *J. Comput. Sci. Syst. Biol.*, vol. 9, no. 4, pp. 119–124, 2016.
[6] *Radiofrequency and Health: A Summary*. Accessed: Oct. 13, 2020. [Online]. Available: https://www2.gov.bc.ca/assets/gov/health/about-bc-s-health-care-system/office-of-the-provincial-health-officer/radiofrequency-summary.pdf
[7] A. Ahlbom, A. Green, L. Kheifets, D. Savitz, and A. Swerdlow, "Epidemiology of health effects of radiofrequency exposure," *Environ. Health Perspect.*, vol. 112, no. 17, pp. 1741–1754, Dec. 2004.
[8] K. S. Tan, I. Hinberg, and J. Wadhwani, "Electromagnetic interference in medical devices: Health Canada's past and current perspectives and activities," in *Proc. IEEE Int. Symp. Electromagn. Compat.*, Aug. 2001, pp. 1283–1284.
[9] N. Saeed, S. Guo, K. H. Park, T. Y. Al-Naffouri, and M. S. Alouini, "Optical camera communications: Survey, use cases, challenges, and future trends," *Phys. Commun.*, vol. 37, pp. 1–17, Dec. 2019.
[10] W. Huang, P. Tian, and Z. Xu, "Design and implementation of a real-time CIM-MIMO optical camera communication system," *Opt. Express*, vol. 24, pp. 24567–24579, Oct. 2016.
[11] M. Hasan, M. Shahjalal, M. Chowdhury, and Y. Jang, "Real-time healthcare data transmission for remote patient monitoring in patch-based hybrid OCC/BLE networks," *Sensors*, vol. 19, no. 5, p. 1208, Mar. 2019.
[12] M. Z. Chowdhury, M. T. Hossan, M. Shahjalal, M. K. Hasan, and Y. M. Jang, "A new 5G eHealth architecture based on optical camera communication: An overview, prospects, and applications," *IEEE Consum. Electron. Mag.*, vol. 9, no. 6, pp. 23–33, Nov. 2020.
[13] Z. Ong, V. P. Rachim, and W.-Y. Chung, "Novel electromagnetic-interference-free indoor environment monitoring system by mobile camera-image-sensor-based VLC," *IEEE Photon. J.*, vol. 9, no. 5, pp. 1–11, Oct. 2017.

[14] M. F. Ahmed, M. K. Hasan, M. Shahjalal, M. M. Alam, and Y. M. Jang, "Experimental demonstration of continuous sensor data monitoring using neural network-based optical camera communications," *IEEE Photon. J.*, vol. 12, no. 5, pp. 1–11, Oct. 2020.
[15] O. I. Younus, H. Le Minh, P. T. Dat, N. Yamamoto, A. T. Pham, and Z. Ghassemlooy, "Dynamic physical-layer secured link in a mobile MIMO VLC system," *IEEE Photon. J.*, vol. 12, no. 3, pp. 1–14, Apr. 2020.
[16] W. A. Cahyadi, Y. H. Kim, Y. H. Chung, and C.-J. Ahn, "Mobile phone camera-based indoor visible light communications with rotation compensation," *IEEE Photon. J.*, vol. 8, no. 2, pp. 1–8, Apr. 2016.
[17] G. Wang, S. Zhang, S. Dong, D. Lou, L. Ma, X. Pei, H. Xu, U. Farooq, W. Guo, and J. Luo, "Stretchable optical sensing patch system integrated heart rate, pulse oxygen saturation, and sweat pH detection," *IEEE Trans. Biomed. Eng.*, vol. 66, no. 4, pp. 1000–1005, Apr. 2019.
[18] J. Hernandez, D. McDuff, K. Quigley, P. Maes, and R. W. Picard, "Wearable motion-based heart rate at rest: A workplace evaluation," *IEEE J. Biomed. Health Informat.*, vol. 23, no. 5, pp. 1920–1927, Sep. 2019.
[19] B. Venema, N. Blanik, V. Blazek, H. Gehring, A. Opp, and S. Leonhardt, "Advances in reflective oxygen saturation monitoring with a novel in-ear sensor system: Results of a human hypoxia study," *IEEE Trans. Biomed. Eng.*, vol. 59, no. 7, pp. 2003–2010, Jul. 2012.
[20] W.-T. Sung, J.-H. Chen, and K.-W. Chang, "Mobile physiological measurement platform with cloud and analysis functions implemented via IPSO," *IEEE Sensors J.*, vol. 14, no. 1, pp. 111–123, Jan. 2014.
[21] O. S. Alwan and K. Prahald Rao, "Dedicated real-time monitoring system for health care using ZigBee," *Healthcare Technol. Lett.*, vol. 4, no. 4, pp. 142–144, Aug. 2017.
[22] V. P. Tran and A. A. Al-Jumaily, "A novel oxygen-hemoglobin model for non-contact sleep monitoring of oxygen saturation," *IEEE Sensors J.*, vol. 19, no. 24, pp. 12325–12332, Dec. 2019.
[23] J. Wannenburg and R. Malekian, "Body sensor network for mobile health monitoring, a diagnosis and anticipating system," *IEEE Sensors J.*, vol. 15, no. 12, pp. 6839–6852, Dec. 2015.
[24] D. Shao, C. Liu, F. Tsow, Y. Yang, Z. Du, R. Iriya, H. Yu, and N. Tao, "Noncontact monitoring of blood oxygen saturation using camera and dual-wavelength imaging system," *IEEE Trans. Biomed. Eng.*, vol. 63, no. 6, pp. 1091–1098, Jun. 2016.

MD. FAISAL AHMED (Graduate Student Member, IEEE) received the B.Sc. degree in electrical and electronic engineering (EEE) from the Khulna University of Engineering & Technology (KUET), Bangladesh, in 2019. He is currently pursuing the M.Sc. degree in electronics engineering with the Wireless Communication and Artificial Intelligence Laboratory, Kookmin University, South Korea. His research interests include optical wireless communications (OWC), optical camera communication (OCC), convolutional neural network (CNN), wireless power transfer (WPT), the IoT in a smart home, 5G, and 6G.

MOH. KHALID HASAN (Member, IEEE) received the B.Sc. degree in electrical and electronic engineering (EEE) from the Khulna University of Engineering & Technology (KUET), Khulna, Bangladesh, in May 2017, and the M.Sc. degree in electronics engineering from Kookmin University, South Korea, in August 2019. Since September 2019, he has been a full-time Researcher with the Wireless Communications and Artificial Intelligence Laboratory, Department of Electronics Engineering, Kookmin University. His current research interests include wireless communications, 6G, wireless security, and artificial intelligence. He received the Academic Excellence Award from Kookmin University, in 2019, for his research.

MD. SHAHJALAL (Student Member, IEEE) received the B.Sc. degree in electrical and electronic engineering (EEE) from the Khulna University of Engineering & Technology (KUET), Bangladesh, in May 2017, and the M.Sc. degree in electronics engineering from Kookmin University, South Korea, in August 2019, where he is currently pursuing the Ph.D. degree in electronics engineering. His research interests include optical wireless communications, wireless security, non-orthogonal multiple access, the Internet of Things, low-power wide-area networks, and 6G mobile communications. He received the Excellent Student Award from Kookmin University.

MD. MORSHED ALAM (Graduate Student Member, IEEE) received the B.Sc. degree in electrical and electronic engineering (EEE) from the Khulna University of Engineering & Technology (KUET), Bangladesh, in May 2018. He completed Exchange Program on power system from the University of Porto, Portugal, in September 2017. He is currently pursuing the M.Sc. degree in electronics engineering with the Wireless Communication and Artificial Intelligence Laboratory, Kookmin University, South Korea. His research interests include smart grid, micro-grid, renewable energy, power control and stability, artificial intelligence (AI), and machine learning (ML).

YEONG MIN JANG (Member, IEEE) received the B.E. and M.E. degrees in electronics engineering from Kyungpook National University, South Korea, in 1985 and 1987, respectively, and the Ph.D. degree in computer science from the University of Massachusetts, USA, in 1999. From 1987 to 2000, he was with the Electronics and Telecommunications Research Institute (ETRI). Since 2002, he has been with the School of Electrical Engineering, Kookmin University, Seoul, South Korea, where he has been the Director of the Ubiquitous IT Convergence Center, from 2005 to 2010, the Director of the LED Convergence Research Center, since 2010, and the Director of the Internet of Energy Research Center, since 2018. He is currently a Life Member of the Korean Institute of Communications and Information Sciences (KICS). His research interests include 5G/6G mobile communications, the Internet of Energy, eHealth, multiscreen convergence, public safety, optical wireless communications, optical camera communication, and the Internet of Things (IoT). He has organized several conferences and workshops, such as the International Conference on Ubiquitous and Future Networks, from 2009 to 2017, the International Conference on ICT Convergence, from 2010 to 2016, the International Conference on Information Networking 2015, and the International Workshop on Optical Wireless LED Communication Networks, from 2013 to 2016. He received the Young Science Award from the Korean Government, during 2003–2006. He had served as the Founding Chair of the KICS Technical Committee on Communication Networks, in 2007 and 2008. He had served as the Executive Director of KICS, from 2006 to 2014, the Vice President of KICS, from 2014 to 2016, and the Executive Vice President of KICS, since 2018. He serves as the Co-Editor-in-Chief of ICT Express, which is published by Elsevier. He had been the Steering Chair of the Multi-Screen Service Forum, since 2011, and the Society Safety System Forum, since 2015. He had served as the Chairman of the IEEE 802.15 Optical Camera Communications Study Group, in 2014. He is currently serving as the Chairman of the IEEE 802.15.7m Optical Wireless Communications Task Group. He is also the Chairman of the IEEE 802.15 Vehicular Assistive Technology (VAT) Interest Group.